Phycologia Volume 56 (5), 533–548 Published 20 June 2017

Studies on woloszynskioid dinoflagellates VIII: life cycle, resting cyst morphology and phylogeny of *Tovellia rinoi sp. nov.* (Dinophyceae)

Mariana S. Pandeirada[1,2], Sandra C. Craveiro[1,2]*, Niels Daugbjerg[3], Øjvind Moestrup[3] and António J. Calado[1,2]

[1]*Department of Biology, University of Aveiro, P-3810-193 Aveiro, Portugal*
[2]*GeoBioTec Research Unit, University of Aveiro, P-3810-193 Aveiro, Portugal*
[3]*Marine Biological Section, Department of Biology, University of Copenhagen, Universitetsparken 4, DK-2100 Copenhagen Ø, Denmark*

Abstract: *Tovellia rinoi nov. sp.* is described on the basis of light microscopic and scanning electron microscopic examination of motile cells and resting cysts and the phylogenetic analysis of partial sequences of the large subunit ribosomal rRNA gene. The species was isolated from a flooded area near Aveiro, Portugal, and followed in culture through all stages of the life cycle, including formation of vegetative cells and gametes, sexual fusion, planozygote division through division cysts and the production of resting cysts. Motile cells had an ovate-conical epicone and a truncated or slightly excavated hypocone and were a little flattened dorsoventrally. Cell length was mostly 9–19 μm, the smaller cells less pigmented and with the potential to act as gametes but also capable of vegetative multiplication. The amphiesma had three series of vesicles on the epicone, one in the cingulum and two on the hypocone and an apical line of plates (ALP) oriented almost dorsoventrally across the cell apex. One vesicle separated the ALP from the cingulum on the ventral side, two on the dorsal side. The resting cysts, showing an equatorial constriction and densely covered by hair-like spines, represented a new type within the family Tovelliaceae. The new species formed a well-supported sister group to the other *Tovellia* species in a LSU rDNA–derived phylogeny. Sexual fusion started with gametic contact within 'dancing groups' of small cells. The initial contact on the mid-ventral side of both gametes was often visible as a hyaline bridge, which apparently involved a globular structure protruding from the ventral ridge of one or both gametes. The two gametes in a fusing pair behaved differently, with one gamete rotating as it fused into its partner until gametic eyespots merged and the gametic longitudinal flagella assumed the position of the paired longitudinal flagella of the planozygote. Resting cysts developed from large cells morphologically identifiable as planozygotes, with cyst spines growing rapidly. Conversion of planozygotes into division cysts that produced motile cells was also observed. Germinating cysts produced regularly two motile cells, each apparently with a single longitudinal flagellum. Nuclear cyclosis was not detected at any stage of the life cycle.

Key Words: Dinoflagellates, Life cycle, LSU rDNA, Phylogeny, Resting cyst, Tovelliaceae

INTRODUCTION

The genus *Tovellia* Moestrup, K.Lindberg & Daugbjerg was established to accommodate six species of woloszynskioids that shared three distinctive features: a lipidic eyespot not associated with a chloroplast lobe (later designated eyespot type C by Moestrup & Daugbjerg 2007), a row of linear vesicles that cross the anterior part of the epicone accompanied on both sides by a row of narrow amphiesmal vesicles (termed apical line of plates [ALP]) and a resting cyst with a narrow equatorial constriction bordered by protuberances or short spines and usually with horn-like processes in the poles (Lindberg *et al.* 2005). Two recently described species, *Tovellia aveirensis* Pandeirada, Craveiro, Daugbjerg, Moestrup & Calado and *T. paldangensis* Zhun Li, M.S.Han & H.H.Shin, added to the known range of resting cyst morphologies by showing a more even distribution of thick spines on an otherwise smooth, equatorially constricted cyst wall (Pandeirada *et al.* 2014; Li *et al.* 2015). Resting cysts with axial horns, warty lateral bumps and equatorial constriction were reported from *Opisthoaulax* Calado, a genus segregated from the asymmetric *Katodinium* Fott to include heterotrophic freshwater species with a type C eyespot and tovelliacean characteristics in the flagellar and pusular systems (Calado 2011). Other members of the Tovelliaceae, of the genera *Jadwigia* Moestrup, K.Lindberg & Daugbjerg and *Esoptrodinium* Javornický (possibly a synonym of *Bernardinium* Chodat), produce round and smooth resting cysts (Lindberg *et al.* 2005; Calado *et al.* 2006).

A culture strain started from a small cell collected in a flooded area near the city of Aveiro, Portugal, revealed characters that place it in the genus *Tovellia*. The culture batches displayed abundant sexual reproduction and resting cysts were commonly produced. Light microscopic (LM) and scanning electron microscopic (SEM) examination of both the motile cells and the resting cysts showed differences from previously described species. Partial LSU rDNA–based phylogeny supported the description of this strain as a new species of *Tovellia*. This is, after *T. aveirensis*, the second species of *Tovellia* to be reported from Portugal (Pandeirada *et al.* 2013, 2014).

Culture-based studies on the life cycle of dinoflagellates have revealed a much greater versatility than previously recognised, with different strategies adapted to environmental features (e.g. Kremp 2013; Warns *et al.* 2013). Previous

* Corresponding author (scraveiro@ua.pt).
DOI: 10.2216/17-5.1

knowledge on the life cycle of *Tovellia* species comes mainly from the seminal work of Stosch (1973). Limited information on cell division and resting cyst differentiation was provided for *T. aveirensis* (Pandeirada *et al*. 2014). The events leading to vegetative division and gamete formation, sexual fusion, planozygote formation and its alternative routes of development, cyst origin and morphology were examined in cultures of the new species described herein.

MATERIAL AND METHODS

Tovellia rinoi was isolated from the plankton of Ribeiro da Palha (40°33.240′N, 8°34.095′W), a flooded area near the village of Nariz, Aveiro, Portugal, on 15 July 2014. A culture was started from a single, small swimming cell into MBL culture medium (Nichols 1973) and grown at 18°C with 12:12 light:dark photoperiod and photon flux density about 25 μmol m^{-2} s^{-1}. Sexual reproduction has regularly occurred in the culture with abundant production of resting cysts. Several stages of the life cycle were examined by isolating and following haploid swimming cells, fusing pairs and resting cysts in different wells of culture plates (Sarstedt, Numbrecht, Germany). To promote cyst germination, plates with isolated cysts were wrapped in foil and kept at 4°C for about 4 wk.

Swimming cells and resting cysts were photographed with a Zeiss Axioplan 2 *imaging* light microscope (Carl Zeiss, Oberkochen, Germany), equipped with a DP70 Olympus camera (Olympus Corp., Tokyo, Japan). Stages in the life cycle were recorded with a JVC TK-C1481BEG color video camera (Norbain SD Ltd, Reading, UK), mounted either on the Zeiss Axioplan 2 *imaging* or on a Leitz Labovert FS inverted light microscope (Leica Microsystems, Wetzlar, Germany).

Several of the fixation schedules attempted for scanning electron microscopy (SEM) resulted in poor preservation of the cells. All SEM images shown here are from cells processed through the following three schedules. Good preservation of cell shape and flagella was obtained in cells fixed for 5 min with OsO_4 at final concentrations of either 0.1% or 0.5%, made by mixing appropriate volumes of 2% OsO_4 and culture. Visualisation of amphiesmal vesicles was best in cells fixed in 0.2% glutaraldehyde for about 10 min. Fixed material was filtered through Nuclepore polycarbonate filters, 5-μm pore size (Whatman, GE Healthcare Life Sciences, Maidstone, UK), and washed with distilled water for about 40 min. The filters were then dehydrated through a graded ethanol series and critical point dried in a Baltec CPD-030 (Balzers, Liechtenstein). Dried filters were glued onto stubs, sputter coated with gold-palladium and examined with a Hitachi S-4100 (Hitachi High-Technologies Corp., Tokyo, Japan) scanning electron microscope. Resting cysts were fixed in 2% OsO_4 (final concentration) for 15 min and otherwise processed in a similar way.

Groups of five swimming cells were transferred to 0.2-ml PCR tubes and immediately frozen at –8°C for about a week. Following the addition of primers and a bead of illustra puReTaq Ready-To-Go PCR (GE Healthcare, UK Ltd, Buckinghamshire, UK), PCR amplifications were conducted in a Biometra–Tprofessional thermocycler (Biometra GmbH, Göttingen, Germany). The primers and thermal profiles were the same as in Pandeirada *et al*. (2014). The PCR products were loaded on a 1% agarose gel, run for 20 min at 90 V and revealed through a UV light table (Molecular imager chemiDoc XRS System, Bio-Rad Laboratories, Inc., Hercules, California USA). The amount of PCR products was increased through nested PCR using 1 μl of the first PCR products and the following primer combinations: D1R with D3B and D3A with 28-1483 (for primer sequences, see Scholin *et al*. 1994; Nunn *et al*. 1996; Daugbjerg *et al*. 2000). The thermal profile comprised one cycle of denaturation at 94°C for 3 min followed by 18 cycles of each of the next steps: denaturation at 94°C for 1 min, annealing at 52°C for 1 min, extension at 72°C for 3 min and the final cycle of extension at 72°C for 6 min. The sequence reaction products were purified using the QIAquick PCR Purification Kit (Qiagen, Hilden, Germany) following the manufacturer's recommendations and sent to Macrogen Europe (Amsterdam, Netherlands) for sequence determination in both directions. The sequencing primers were the same as in Pandeirada *et al*. (2014).

The partial LSU rDNA sequence of *T. rinoi* (*c*. 1400 base pairs) was aligned with 76 other dinoflagellate species (representing 48 different genera) including all taxa belonging to the Tovelliaceae with available sequences. Due to a high divergence of D2, this domain was deleted before the phylogenetic analyses were conducted. Jalview v14 (Waterhouse *et al*. 2009) was used for sequence alignment based on Clustal W as included in the program. Manual deletion of domain D2 was based on the secondary structure model proposed Lenaers *et al*. (1989). We used MrBayes v3.2.2 x64 (Ronquist & Huelsenbeck 2003) for Bayesian (BA) and PhyML v3.0 (Guindon *et al*. 2010) for maximum likelihood (ML) analyses. In BA, we used 5 million generations; a tree was sampled every 1000 generations, and the analysis was run on a local computer. To evaluate the burn-in value, LnL values were plotted as a function of generations in a spreadsheet. The burn-in occurred after 501,000 generations (conservative estimate); thus, 501 trees were removed, leaving 4500 trees for generating a 50% majority-rule consensus tree in PAUP*, v4.0b10 (Swofford 2003). For analysis with ML, parameter settings obtained from jModelTest v2.1.7 (Darriba *et al*. 2012) were applied. Among the models examined, jModelTest chose GTR+I+G as the best-fit model for the data matrix with a gamma shape = 0.456 and p-invar = 0.14. PhyML was run using the South of France bioinformatics platform, University of Montpellier (Guindon *et al*. 2010). The robustness of the tree topology was evaluated with 1000 bootstrap replications. Three ciliates, four apicomplexans and one perkinsid were used to root the diverse assemblage of dinoflagellates included.

RESULTS

Tovellia rinoi Pandeirada, Craveiro, Daugbjerg, Moestrup & Calado *sp. nov.*

Figs 1–32

DESCRIPTION: Motile vegetative cells with an ovate-conical epicone, sometimes with a slightly projecting ridge formed by the ALP;

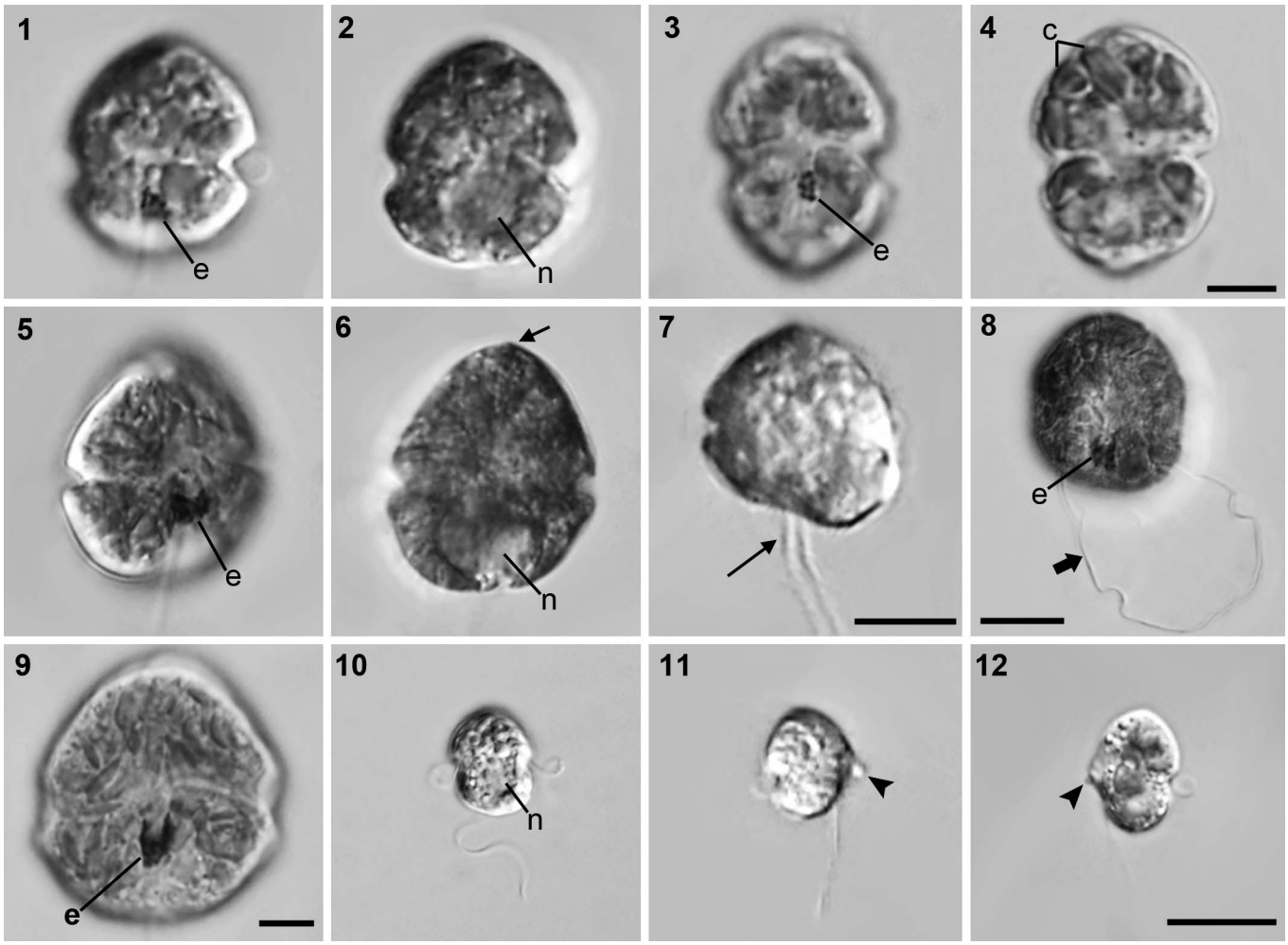

Figs 1–12. *Tovellia rinoi*, motile cells, LM.
Figs 1, 2. Surface focus and optical section of a vegetative cell in ventral view with the typical ovate-conical epicone and a round, slightly shorter hypocone. The eyespot (e) is visible in the sulcus and the round nucleus (n) in the hypocone. Same scale as Fig. 4.
Figs 3, 4. Surface focus and optical section of a cell just released from a division cyst. The eyespot (e) is visibly disconnected from the relatively large chloroplast lobes (c). Scale bar = 5 μm.
Figs 5, 6. Planozygote in different focusing planes with a curved and asymmetrical eyespot resulting from the fusion of the eyespots of the gametes. The epicone is somewhat projected at the level of the ALP (short arrow). Nucleus (n) in the hypocone. Same scale as Fig. 7.
Fig. 7. Planozygote showing paired longitudinal flagella (arrow). Image taken from video recording of the swimming cell. Scale bar = 10 μm.
Fig. 8. Large cell (presumably a zygote) emerging from the shed amphiesma (thick arrow). The eyespot appears composed of two units (e). Scale bar = 10 μm.
Fig. 9. Large cell (presumably a planozygote) with horseshoe-shaped eyespot and numerous thin chloroplast lobes at the surface. Scale bar = 5 μm.
Figs 10–12. Ventral and lateral views of smaller, less pigmented cells. Nucleus (n) extends from hypocone to cell centre. Hyaline globular protuberances are visible at ventral ridge level in Figs 11 and 12 (arrowheads). Fig. 11 taken from video recording. Scale bar = 10 μm.

hypocone shorter than epicone, with truncated or slightly excavated posterior end, except in recently divided cells, which sometimes show a somewhat pointed antapex. Cingulum descending, displaced about one cingulum width. Cells somewhat dorsoventrally compressed with the ventral side of the hypocone obliquely flattened. Length mostly 9–19 μm, rarely up to 26 μm, width 5.5–20 μm, thickness 5–14 μm. Chloroplasts yellowish-green, with numerous lobes visible near the surface (light microscopy). Nucleus rounded or ellipsoid, located in the hypocone of vegetative cells. Eyespot red, trough-shaped, located at or slightly above the middle of the sulcal groove. Amphiesma with large pentagonal or hexagonal vesicles disposed in roughly six latitudinal series: three on the epicone, one in the cingulum and two on the hypocone. Precingular amphiesmal vesicles mostly pentagonal, their aligned posterior edges forming the straight and sharply marked anterior border of the cingulum. Remaining vesicles generally larger, usually roughly hexagonal. Ventral-antapical area with a seven- or eight-sided vesicle that abuts the posterior end of the sulcal groove; this is the largest of the amphiesmal vesicles. The hypocone often shows intercalary vesicles that are not part of the latitudinal series. A line of narrow vesicles (the ALP crosses the apical part of the epicone in a nearly dorsoventral orientation and is separated from the cingulum by a rhomboid vesicle on the ventral side and by two vesicles on the dorsal side. The ALP is bordered on both sides by vesicles that are distinctly narrower than those forming the latitudinal series on the epicone. Sulcus with eight or nine amphiesmal vesicles. Resting cysts with equatorial constriction, covered by hair-like spines. Nuclear-encoded partial LSU rRNA gene sequence = GenBank accession KY676891.

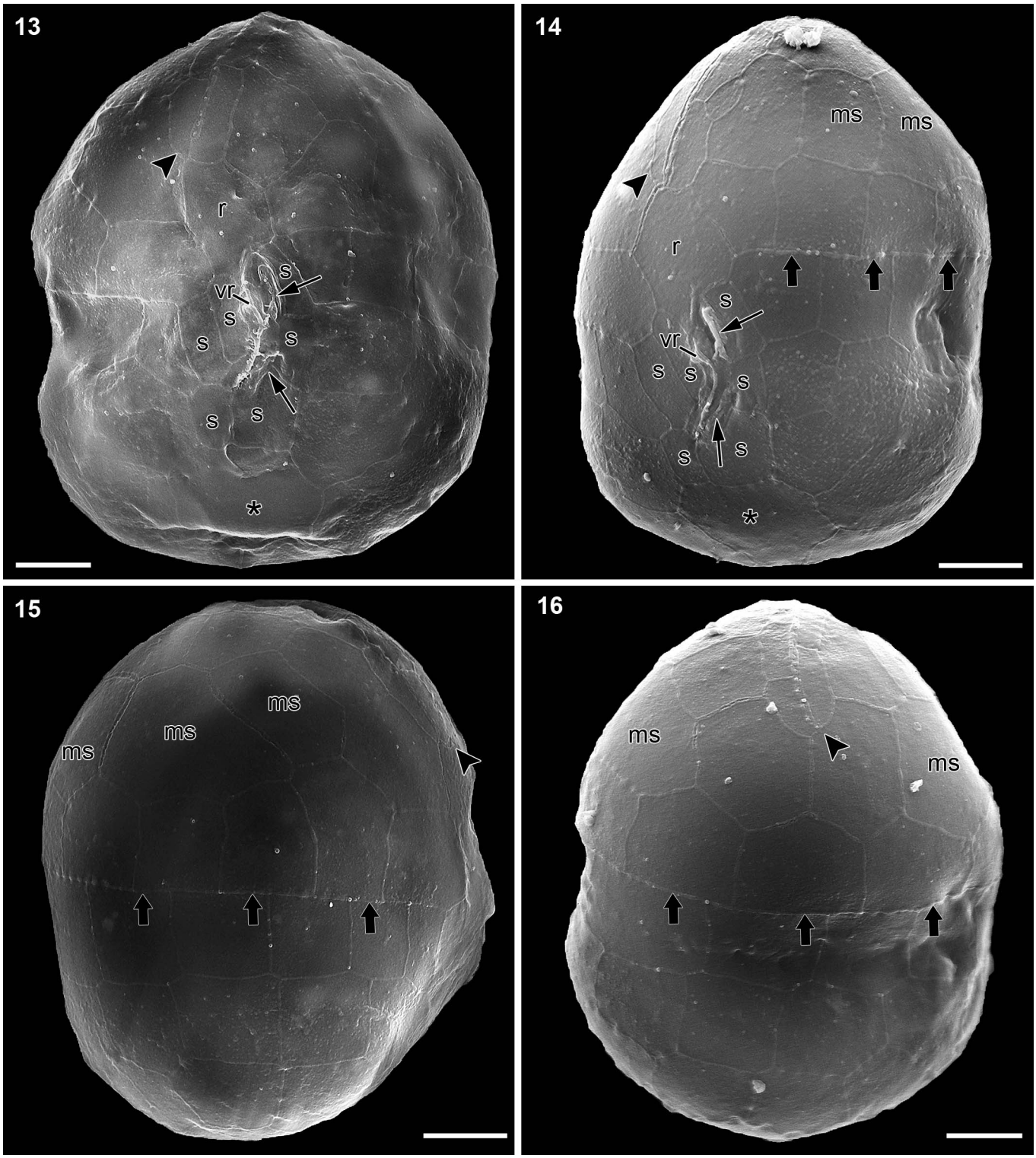

Figs 13–16. *Tovellia rinoi*, motile cells fixed in 0.2% glutaraldehyde, SEM.

Figs 13, 14. Ventral and ventral-left views showing the general arrangement of amphiesmal vesicles. The larger vesicles are arranged in three series in the epicone, one series restricted to the cingulum and two in the hypocone, from the posterior border of the cingulum to the antapex. An ALP bordered by two rows of narrow amphiesmal vesicles (arrowheads) extends toward the apex. An approximately rhombic vesicle (r) separates the ventral tip of the ALP and the sulcal area. The straight anterior edge of the cingulum is marked by thick arrows in Fig. 14. Six vesicles (s) surround flagellar pores (thin arrows) and ventral ridge (vr) in the sulcal area. A prominent seven- or eight-sided vesicle (asterisk) is present near the antapex, adjacent to two vesicles on the posterior end of the sulcus. Two vesicles of the middle series on the epicone are marked (ms) in Fig. 14. Scale bars = 2 μm.

Figs 15, 16. Right-lateral and dorsal views. The anterior edge of the cingulum is marked by arrows. Ventral end of ALP marked by arrowhead in Fig. 15; dorsal end indicated by arrowhead in Fig. 16. ms, middle series vesicles. Scale bars = 2 μm.

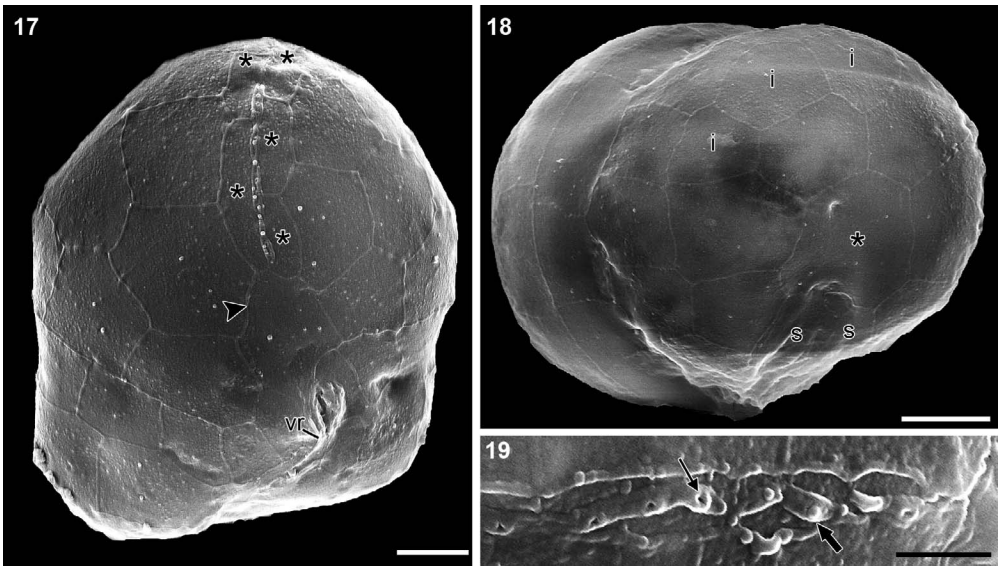

Figs 17–19. *Tovellia rinoi*, motile cells fixed in 0.2% glutaraldehyde, SEM.
Fig. 17. Ventral-apical view showing the ALP bordered by two rows of narrow vesicles (asterisks). vr, ventral ridge. Scale bar = 2 μm.
Fig. 18. Nearly antapical view with a series of vesicles arranged around a larger vesicle (asterisk) that contacts sulcal vesicles (s) on the ventral side. Three posterior intercalary vesicles (i) are visible on the dorsal side. Scale bar = 2 μm.
Fig. 19. Detail of the ALP, showing some of the axial row of knobs (thick arrow) and some of the underlying pores (thin arrow). Scale bar = 0.5 μm.

HOLOTYPE: SEM stub with critical-point-dried cells grown in culture (started from a single cell) and fixed in 0.2% glutaraldehyde. Cells on this stub were somewhat swollen and showed the limits of amphiesmal vesicles clearly. Deposited at the University of Aveiro Herbarium, registered as AVE-A-T-6. Figs 13–19 illustrate cells from this stub.

ISOTYPE: SEM stub with critical-point-dried cells from the same culture strain as the holotype, fixed in 2% OsO_4. This batch contained cysts in several stages of development, including those illustrated by Figs 30–32. Deposited at the University of Aveiro Herbarium, registered as AVE-A-T-7.

TYPE LOCALITY: Temporarily flooded area of the freshwater Ribeiro da Palha near the village of Nariz, Aveiro, Portugal (40°33.240′N, 8°34.095′W), sampled on 15 July 2014.

ETYMOLOGY: The epithet *rinoi* commemorates Jorge Manuel E. Almeida Rino, former professor of phycology at the University of Aveiro and author of a series of important contributions to our knowledge of the continental algae of Portugal and of Mozambique.

General morphology of swimming cells

The general features of motile cells are shown in LM in Figs 1–12, in SEM in Figs 13–21 and in a series of schematic drawings

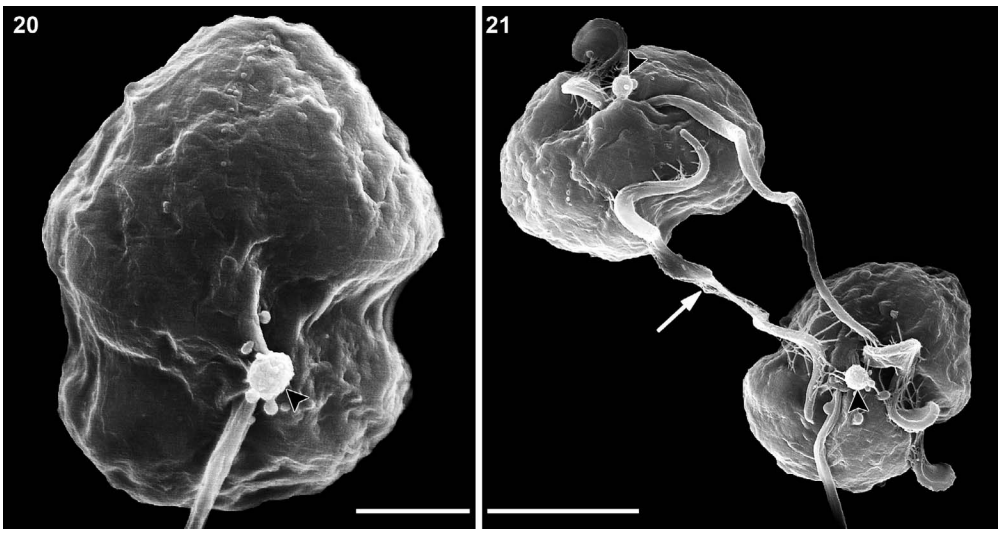

Figs 20, 21. *Tovellia rinoi*, motile cells fixed with 0.1% OsO_4, SEM. Small, gamete-like cells with globose bodies protruding from the ventral ridge (arrowheads). The flagellum-like structure marked with an arrow appears not to belong to any of the cells shown. Scale bar = 2 μm in Fig. 20 and 5 μm in Fig. 21.

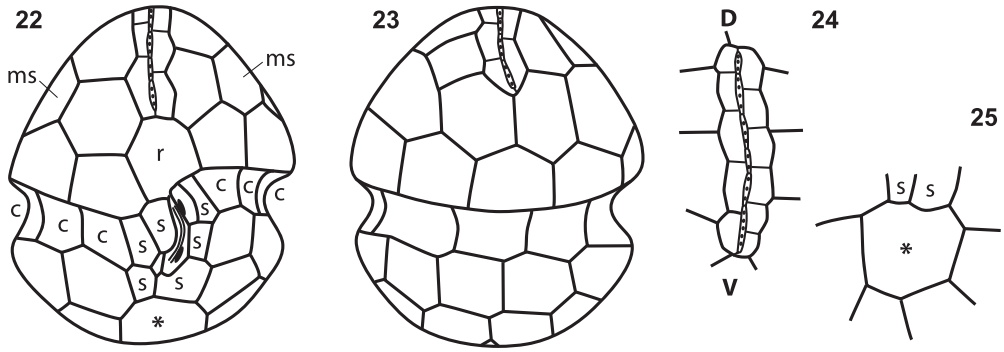

Figs 22–25. *Tovellia rinoi*, schematic drawings showing cell shape and arrangement of amphiesmal vesicles.
Figs 22, 23. Ventral and dorsal views. The large ventral-antapical vesicle (asterisk) contacting sulcal vesicles (s) on the ventral side is marked in Fig. 22. Cingular vesicles marked with 'c', approximately rhombic vesicle on the ventral tip of the ALP labeled 'r' and laterally located vesicles of the middle series marked 'ms'.
Fig. 24. ALP formed by linear vesicles with an axial row of knobs and flanked by two rows of narrow vesicles. Contacts with regular amphiesmal vesicles of the epicone outlined. V, ventral side; D, dorsal side.
Fig. 25. Antapical end of the cell showing the contacts of the large ventral-antapical vesicle (asterisk). The ventral side is marked by two sulcal vesicles (s).

in Figs 22–25. The cells were oval to roughly pentagonal in ventral view, typically with a straight or slightly indented posterior end (Figs 1, 2, 5, 6). In contrast, cells recently emerged from division cysts often showed a somewhat pointed antapex (Figs 3, 4). The ALP was just visible in LM as a thin pointed projection on the apical outline of the cell (Fig. 6). The cingulum was located slightly below the middle and descended about one cingulum width near its right-hand, distal end (Figs 5, 9, 13, 14, 17, 20). Cells were somewhat flattened dorsoventrally, and in side view the ventral side of the hypocone receded obliquely from cingulum level toward the antapex (Figs 11, 12, 15). Cell length and width were 9–19(–26) μm and 6–20 μm, respectively ($n = 45$ for both measures), and thickness was 5–14 μm ($n = 30$). Only four cells were found to be longer than 19 μm. Chloroplasts were visible as yellowish-green discs and ribbons at the cell periphery; a slightly more radial arrangement of chloroplasts was seen in some recently divided cells (Fig. 4), but an attachment of peripheral lobes to a central pyrenoid was not discernible in LM. The nucleus was round to elliptical and located in the hypocone (Figs 2, 6), sometimes extending to the middle of smaller cells (Fig. 10). The bright-red eyespot had the appearance and location that is commonly seen in type C eyespots, and no connection to a chloroplast lobe could be established in LM; it is therefore interpreted as extraplastidial. The aggregate of red, round bodies that make up the eyespot of a cell recently released from a division cyst is shown in Fig. 3. Cells appearing to have two eyespots close together or a wider eyespot with the appearance of two connected eyespots were common in culture (Figs 5, 8, 9). Some of these cells with larger, and nearly horseshoe-shaped eyespots had two longitudinal flagella and were interpreted as planozygotes (Figs 5, 7, 9). Some cells showed a hyaline, globular protuberance on the mid-ventral side; these cells were usually among the smallest and least pigmented and were interpreted as potential gametes (see below) (Figs 11, 12).

Structure of the amphiesma

In Fig. 8 (arrow), the amphiesma shed by a large cell is visible as a relatively robust theca, indicating the presence of thin plates in the amphiesmal vesicles of the type shown for other species of *Tovellia* (Lindberg *et al.* 2005; Pandeirada *et al.* 2014). The major amphiesmal vesicles were arranged in more or less regular latitudinal series, three on the epicone, two on the hypocone and one series confined to the upper side of the cingulum (Figs 13–16). The anterior edge of the cingulum was sharply defined by the sutures between precingular and cingular vesicles; whereas, the posterior border of the cingulum was more round and was lined by both the posterior sides of cingular and the anterior sides of postcingular vesicles (Figs 14–16). Vesicles referable to the middle series on the epicone were usually larger, often forming an incomplete series on the cell's dorsal side (Fig. 16). However, a line drawn from cingulum to apex on the right and left sides of the cell would regularly cross three vesicles (Figs 14, 15, 17). A straight or slightly curved row of about six narrow vesicles (the ALP) extended from ventral to dorsal across the cell apex; the vesicles were 0.3–1.2 μm long ($n = 10$) and 0.1–0.3 μm wide ($n = 20$) and showed an axial row of knobs or open pores (Figs 17, 19). The ALP was lined by about a dozen vesicles 1.0–3.5 μm long and 0.3–1.0 μm wide ($n = 22$). The ALP was separated from the cingular-sulcal area by an approximately rhombic vesicle (Figs 13, 14, 17). Two vesicles separated the cingulum from the dorsal end of the ALP (Fig. 16). The two series of vesicles on the hypocone were roughly arranged around a larger, seven- or eight-sided vesicle located on the ventral side of the antapex, next to the sulcus (Figs 13, 14, 18, asterisk). A group of intercalary vesicles was usually present on the dorsal side of the hypocone (Fig. 18). In the sulcal area, six vesicles could be recognised surrounding the flagellar pores (Fig. 13). A ventral ridge extended obliquely along the upper part of the sulcus, rising between the flagellar pores (Figs 13, 14, 17). Globose bodies were found protruding from the ventral ridge

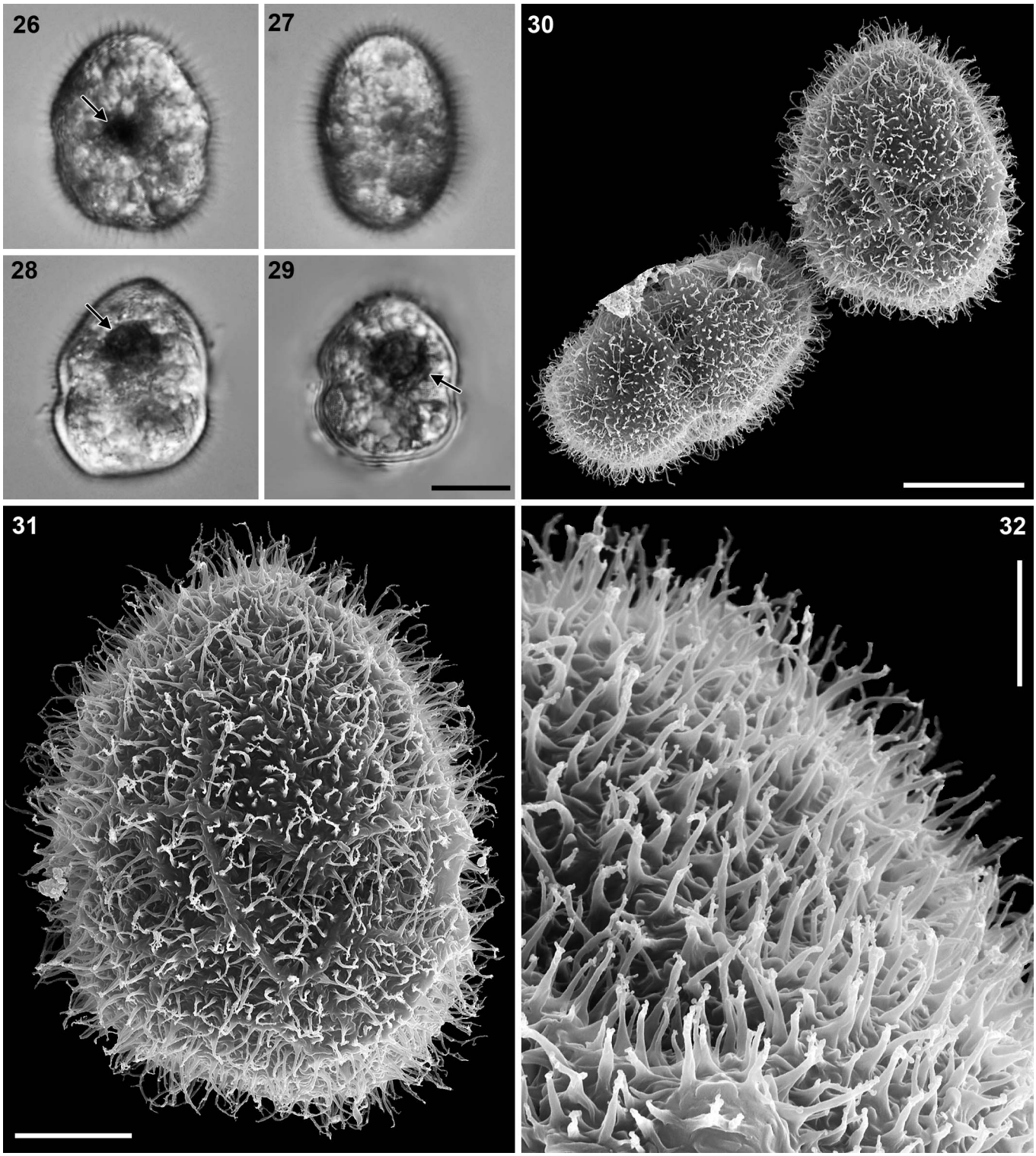

Figs 26–32. *Tovellia rinoi*, resting cysts, LM and SEM.
Figs 26, 27. Frontal and side views of an immature cyst (LM) with thin wall covered by thin, hair-like spines. An accumulation body is seen above the equatorial constriction (arrow). Both figures at the same scale as Fig. 29.
Figs 28, 29. Mature, thick-walled cysts with spiny and smooth surfaces, respectively (LM). Accumulation bodies marked with arrows. Scale bar = 10 μm.
Figs 30, 31. Frontal and lateral views of spiny cysts (SEM). Scale bar = 10 μm in Fig. 30 and 5 μm in Fig. 31.
Fig. 32. Detail of a spiny cyst surface, showing variation in spine tip morphology. Scale bar = 2 μm.

of some small cells, which were regarded as gametes based on their behaviour (Figs 20, 21).

Resting cyst morphology

Resting cysts regularly appeared in the culture batches. They generally resembled swimming cells in outline, with a shallow but distinct furrow marking the position of the cingulum (Figs 26, 28–31). Immature cysts showed a thin wall and extensive yellowish-green chloroplast lobes delimiting some colourless areas (Figs 26, 27). Older cysts had thick walls up to 1.4 μm thick and were largely devoid of recognisable chloroplast lobes (Figs 28, 29). A reddish-brown body was recognisable slightly above the cingulum (paracingulum) level of recently formed cysts and gradually became the only distinctly coloured area of mature cysts (Figs 26, 28, 29). The cyst surface was nearly always densely covered with spines, which developed at early stages of cyst maturation (Figs 26–28); though, apparently smooth cysts were occasionally found (Fig. 29). The spines looked thin and hair-like in LM and were easily missed under low-resolution objectives. Densely spiny cysts are shown in SEM in Figs 30 and 31. Spine length was rather variable, even in the same cyst, and reached a maximum of about 3 μm. Most spines were unbranched, tapering structures, but some had tips slightly enlarged or branched (Fig. 32). Cysts were 21–27 μm long and 15–21 μm wide ($n = 15$).

Life cycle observations: asexual reproduction and gamete formation

Growing cultures always developed division cysts, which were more numerous near the end of both the light and the dark period. Division cysts gave rise to two (Figs 33–36), four (Figs 37–40) or eight cells (Figs 41–44). Cells resulting from division into groups of eight were rather small (*c.* 10 μm long) and somewhat less pigmented than large cells; these small cells resembled those that were seen fusing in the same batches and were therefore interpreted as potential gametes, representing cells in the haploid stage of the population. The development of cysts dividing into eight cells was followed with the microscope, and emergent cells were individually isolated into separate wells. The isolated cells grew for 7–11 d and ended up transforming into division cysts that again formed two, four or eight cells. Not surprisingly, the size of the newly formed cells was smallest for cells formed in groups of eight, which were about the same size as those initially isolated. The new offspring cells produced in pairs, in groups of four and in groups of eight were again isolated into separate culture wells and followed until they turned into division cysts, which this time produced predominantly four cells. The growth period of isolated cells before transforming into division cysts was 3–5 d for cells that had been produced in twos or fours and over 10 d for the small cells that came from groups of eight.

Small, little-pigmented, gamete-like cells were also produced in bulk cultures from division cysts with an initial small size that divided into four cells (Figs 39, 40). Cells transforming into such division cysts had sizes that matched those of cells resulting from larger cysts dividing into two or four cells, thereby suggesting the two-stage formation of gametes as an alternative mechanism to the direct division into eight small cells.

Details of cell division, such as movements of the nucleus and development of cleavage furrows, were similar to those observed during division of planozygotes; they are described below in the context of observations made on these larger cells.

Life cycle observations: gamete fusion

Fusing pairs were commonly established within groups of gametes that swarmed around and hit each other, here called 'dancing groups' following Stosch (1973) (Figs 45, 46). Formation of 'dancing groups' seemed related to photoperiod, as they were more numerous near the end of the light period. Gamete pairs that successfully fused into planozygotes initially attached through their mid-ventral sides at the level of the ventral ridge. During the initial stages of attachment, a hyaline bridge was often visible between the ventral faces of fusing gametes (Figs 47, 48, arrow). At this early stage, the fusing cells were able to turn around the hyaline bridge, thereby changing their relative orientation. The location on the cell surface of the hyaline bridge matched the position of the globular protuberance often glimpsed on the mid-ventral side of small cells and of the globose bodies seen on the ventral ridge with the SEM (Figs 20, 21). Following the initial adjustment period, the gamete pair usually slowed down and appeared to drift for a while; cells sometimes separated at this stage. When fusion continued, the pair often sank to the bottom while rearranging their position and increasing the connection. The pair then resumed swimming with the cells in a distinctively asymmetrical arrangement; one gamete obliquely or perpendicularly positioned across the ventral surface of the epicone of the other (respectively labelled 'a' and 'b' in Figs 49, 51, 53–59). From this point on, propulsion for the swimming pair was provided by the flagella of the lowermost cell (cell 'b'), which seemed to gradually engulf the other gamete over the following half hour (Figs 54–59). The transverse flagellum of cell 'b' was often observed undulating outside the cingulum during cell fusion (Figs 54, 55, 57, thick arrow). The transverse flagellum of cell 'a' was not observable since the early stages of fusion; though, it was not clear whether it was lost or reabsorbed by the cell. In contrast, the longitudinal flagellum of cell 'a' remained in the sulcus, and both the longitudinal flagella and the eyespots of the two gametes converged, apparently through a rotation of cell 'a' as it merged into gamete 'b' (Figs 51, 52; eyespots converging in Figs 54, 58). The two longitudinal flagella were retained in the planozygote, and the eyespots came together, apparently fusing into one (Fig. 60).

Life cycle observations: fate of planozygotes

Abundant resting cysts were found in the culture batches. They resulted from the transformation of large cells that usually displayed a prominent, reddish brown body in the epicone. Large cells developing into resting cysts were found to carry two longitudinal flagella in all cases where this could be verified and were therefore interpreted as large planozygotes, that is, planozygotes that underwent a period of growth. However, cyst formation was not the only observed develop-

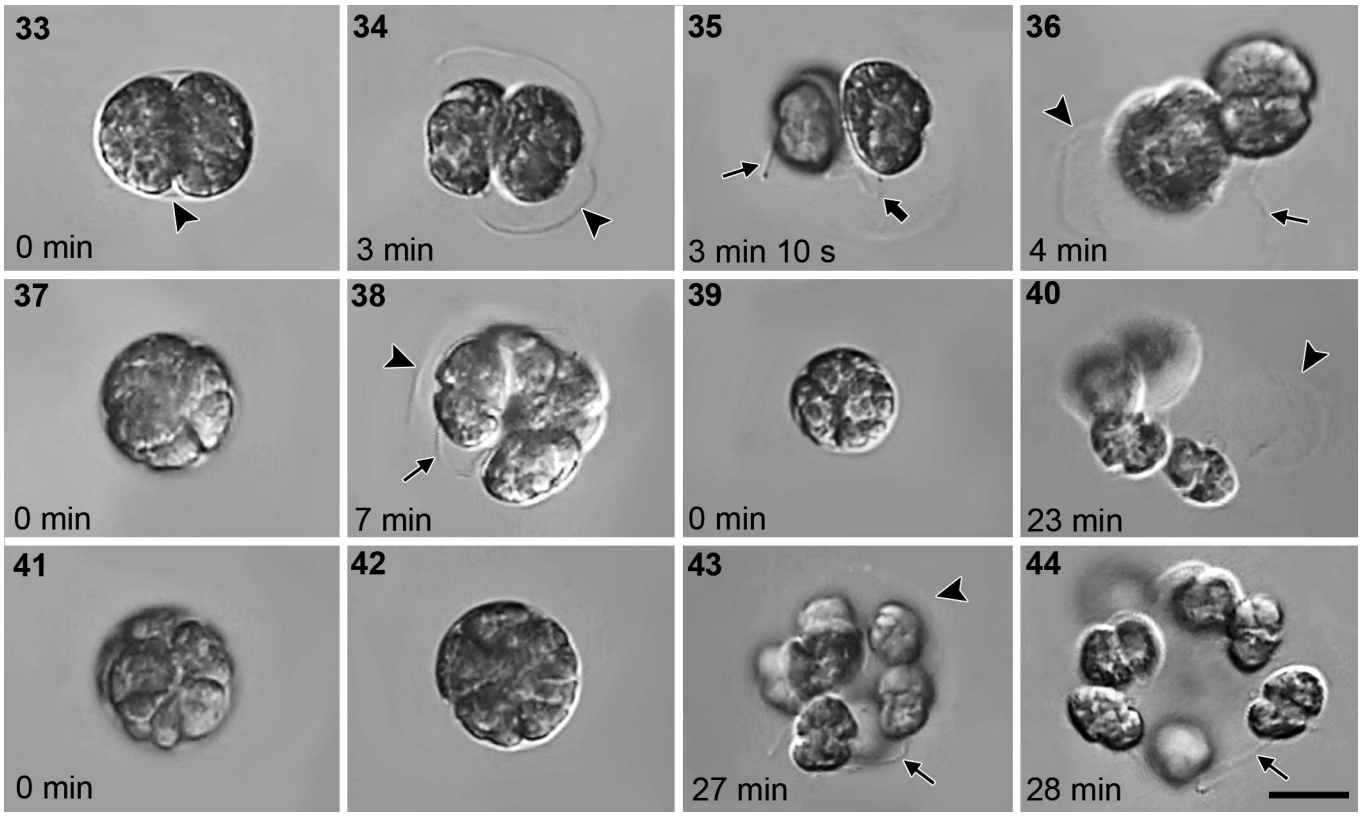

Figs 33–44. *Tovellia rinoi*, asexual reproduction, LM. Image sequences taken from video recordings. The time elapsed is indicated for images within each sequence. Arrowheads mark division cyst covers, the thick arrow in Fig. 35 points to a transverse flagellum and thin arrows indicate longitudinal flagella. Scale bar = 10 μm.

Figs 33–36. Division cyst with two offspring cells being released.

Figs 37–40. Stages in the release of four offspring cells in average-sized (Figs 37, 38) and small (Figs 39, 40) division cysts. Cells released in Fig. 40 are of gamete size.

Figs 41–44. Stages in the release of eight offspring cells in an average-sized division cyst. Cells escaping the cyst are of gamete size.

ment of these cells. Similar-looking larger cells and also somewhat smaller cells carrying two longitudinal flagella were observed in the culture batches to produce division cysts giving rise to two and to four cells. Interestingly, all unequivocal planozygotes obtained by isolating pairs of fusing gametes ended up producing division cysts after a period of enlargement of 5–8 d; four cells emerged from the division cysts in seven out of eight isolates; whereas, the remaining one produced only two. Some of the cells emerging from these division cysts were reisolated into different culture wells, where 4–5 d later they developed into division cysts themselves, producing predominantly four cells. Verification of the number of flagella in cells of these two generations of division cysts was difficult in the cultures; some clearly showed only one longitudinal flagellum, and none seemed to possess two.

The observable events during division were similar for all cells, from gamete-like to planozygote-like (Figs 61–65). Division usually followed the migration of the nucleus to the centre of rounded cells (i.e. with the furrows barely marked) lying on the bottom after losing flagella and outer cell cover (Fig. 61). Division into two cells occurred through a cleavage furrow formed near the cingular area (top cell in Figs 61–65). During division into four cells, it was not clear whether all cells separated simultaneously or in sequence (or whether both processes were possible) (lower cell in Figs 61–65).

Both division and resting cysts were found mainly near the wall of the culture well. The differentiation of resting cyst features from planozygotes isolated into microscope preparations with a drop of MBL medium proved to be a swift process (Figs 66–71). The typical spines were seen to grow out continuously from the cell surface, reaching their maximum length seconds to minutes after the cell left its light theca through the apical area (Figs 68–71). The accumulation bodies seen in planozygotes were maintained in a similar location in the cysts, somewhat above the paracingulum (Fig. 71).

Life cycle observations: cyst germination

Resting cysts directly isolated from culture batches into fresh culture medium sometimes germinated, but more reliable results were obtained after 4 wk in the dark at 4°C. However, signs of imminent germination were not easily detected, making direct observation of germination difficult. In any case, the number of cells found in wells with empty walls of isolated cysts was always two; this included situations in which periodic observations determined that

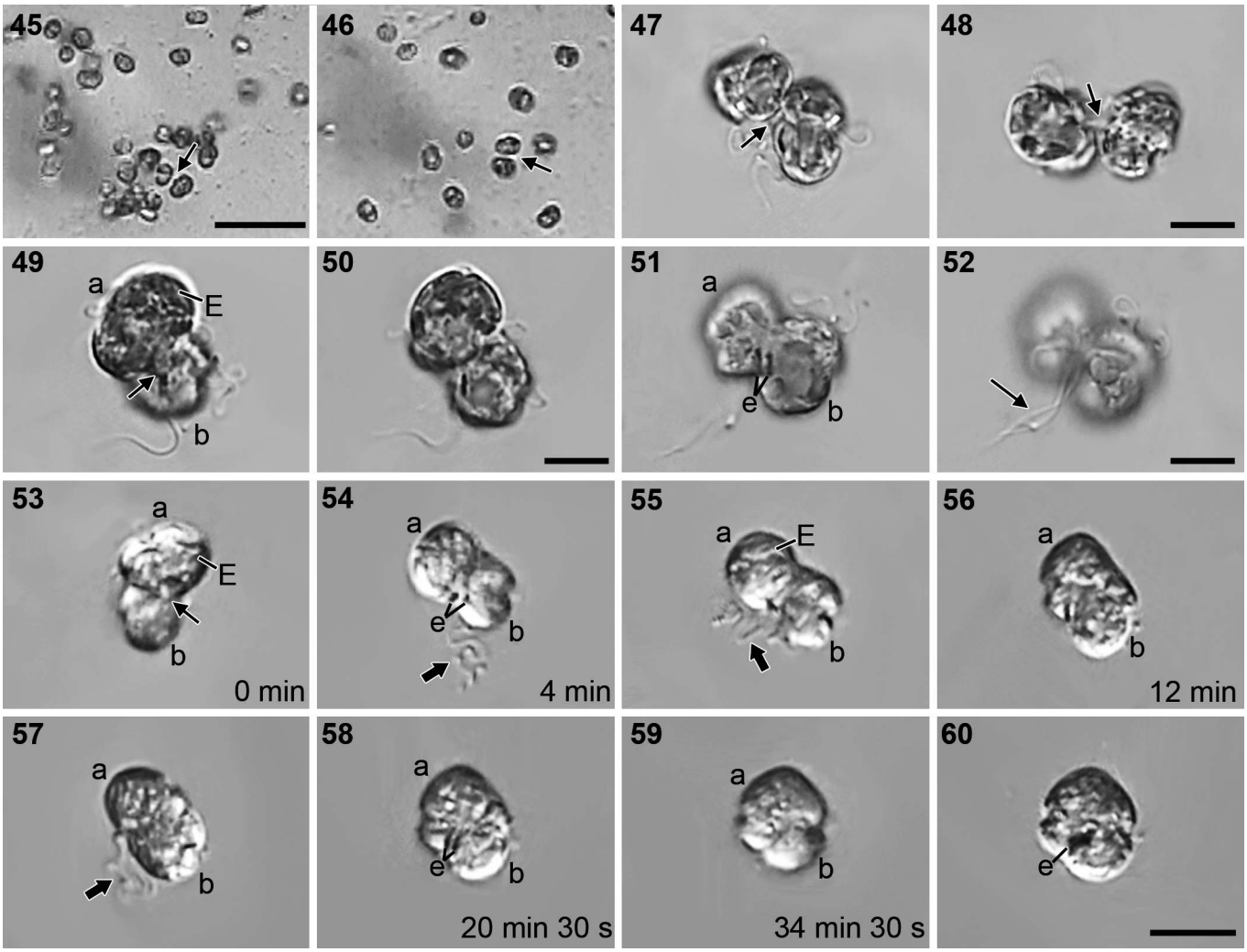

Figs 45–60. *Tovellia rinoi*, sexual reproduction, LM. Images taken from video recordings.
Figs 45, 46. A gamete pair (arrow) established within a 'dancing group'. Scale bar = 50 μm.
Figs 47, 48. Pair of recently connected gametes attached through a hyaline bridge on their mid-ventral sides (arrow). Scale bar = 10 μm.
Figs 49, 50. Pair of gametes at an early stage of fusion. Gamete 'a' is obliquely positioned across the ventral side of the epicone of gamete 'b'. Fusion extends down to the ventral ridge area of gamete 'b', just above the eyespot (arrow in Fig. 49). E, epicone of gamete 'a'. Scale bar = 10 μm.
Figs 51, 52. Early fusion at a slightly later stage than Figs 49 and 50. Eyespots (e) and longitudinal flagella (long arrow) of gametes 'a' and 'b' placed nearly side by side. Scale bar = 10 μm.
Figs 53–60. Sequence of events recorded during the fusion of a single pair of gametes. The time elapsed is indicated in each image (Figs 55 and 57 were taken very shortly after the preceding images). The eyespots (e) gradually approached each other as gamete 'a' turned while merging into gamete 'b'. The transverse flagellum of gamete 'b' (thick arrow) undulated outside the cingulum for most of the process. E, epicone of gamete 'a'. Scale bar = 10 μm.

germination had occurred from minutes to a few hours before. Several cysts were also found to contain two cells (Fig. 72). The possibility of a single cell being occasionally released that would then divide into two could not be ruled out by the observations.

Some of the cells resulting from cyst germination were reisolated and formed division cysts after 4–6 d, which produced four cells. Batches generated from these cells differed greatly in the frequency of resting cyst formation, some showing large numbers; whereas, in others, resting cysts were rarely observed. Similar variation in resting cyst abundance was noted between batches started from isolated haploid, gamete-like cells.

LSU rDNA–based phylogeny of *T. rinoi*

Both BA and ML analyses provided high support for the monophyletic origin of the genus *Tovellia*, with posterior probability (PP) = 1.0 and bootstrap support (BS) =100% (Fig. 73). Within the genus, *T. rinoi* formed the earliest branch and thus appeared as a sister taxon to the remaining species of *Tovellia*. The monophyly of the family Tovelliaceae was highly supported by BA (PP = 1.0) but received only moderate support in ML (BS = 65%) with *Jadwigia applanata* Moestrup, K.Lindberg & Daugbjerg forming a sister taxon to the rest of the Tovelliaceae (*Tovellia* spp. and *Esoptrodinium gemma*). The phylogenetic analysis did not resolve a close relationship

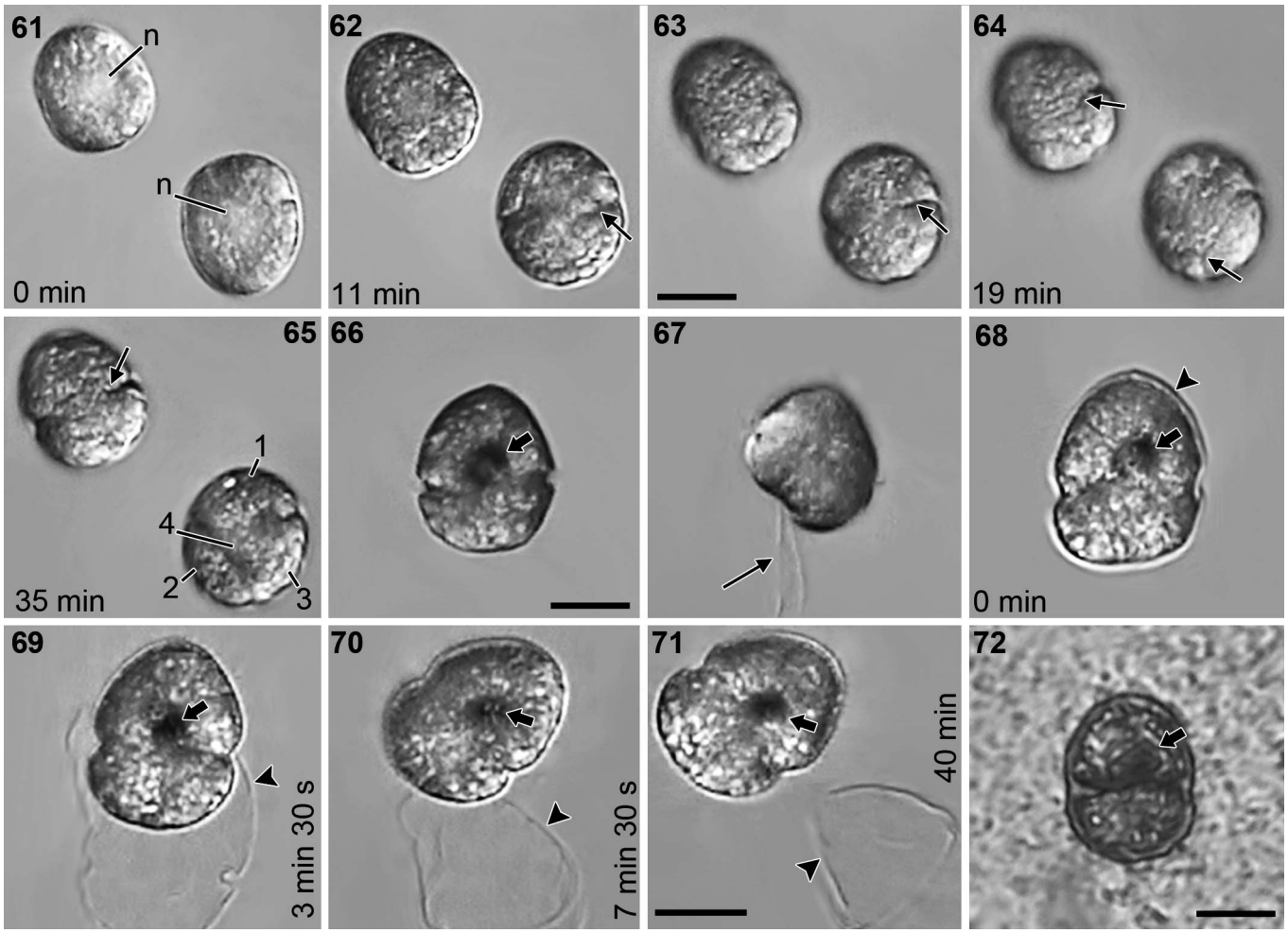

Figs 61–72. *Tovellia rinoi*, division and encystment of large, presumably zygotic cells, LM. Image sequences taken from video recordings. The time elapsed is indicated for images within each sequence.

Figs 61–65. Division of planozygote-derived division cysts into two (top left) and four cells (bottom right). Division started after loss of mobility and migration of the nucleus (n) to the cell centre. Arrows point to cleavage furrows. Figs 62 and 63 show different focusing planes taken in immediate sequence. Numbers in Fig. 65 indicate the four daughter cells. Scale bar = 10 μm.

Figs 66, 67. Planozygote with an accumulation body just above the cingulum (thick arrow) and two longitudinal flagella (thin arrow). The aspect shown corresponds to the stage before loss of motility and encystment. Scale bar = 10 μm.

Figs 68–71. Formation of the resting cyst. About 3 min from settling on the bottom of a slide, the cell exited the outer cover (arrowhead), and the resting cyst spines started to elongate. The accumulation body of the cyst was maintained in the same place as in the planozygote (thick arrow). Scale bar = 10 μm.

Fig. 72. Resting cyst detected on the bottom of a culture well, with the contents divided into two cells. Note the prominent accumulation body in one of the cells (thick arrow). Scale bar = 10 μm.

between Tovelliaceae and any specific dinoflagellate lineage, as the basal part of the tree topology formed a polytomy (Fig. 73).

DISCUSSION

Taxonomic affinities of *T. rinoi* and comparison with related species

Both the LSU rDNA–based phylogeny and the structure of the ALP, with the middle line of narrow vesicles bordered on both sides by a row of amphiesmal vesicles distinctly narrower than the main vesicles on the epicone, mark the known species of *Tovellia* as the closest relatives of *T. rinoi* (Lindberg *et al.* 2005; Pandeirada *et al.* 2014; Li *et al.* 2015). The visible appearance of the prominent eyespot is also compatible with the extraplastidial type seen in the Tovelliaceae.

Ten species were previously assigned to *Tovellia*. Six of these were transferred from the polyphyletic genus *Woloszynskia* (Lindberg *et al.* 2005). Comparative overviews of the features of these six species and some of the more recently described *Tovellia* species are available in Pandeirada *et al.* (2014) and Li *et al.* (2015). The small size and the relatively small number of latitudinal series of vesicles in the amphiesma readily distinguish *T. rinoi* from most other species of the genus. The little-known *T. nygaardii* Moestrup, K.Lindberg & Daugbjerg and the recently described *T. paldangensis* approach *T. rinoi* in number of amphiesmal vesicles and are only slightly larger; however, both *T. nygaardii* and *T. paldangensis* are more rounded, and the very slightly spiraling cingulum of

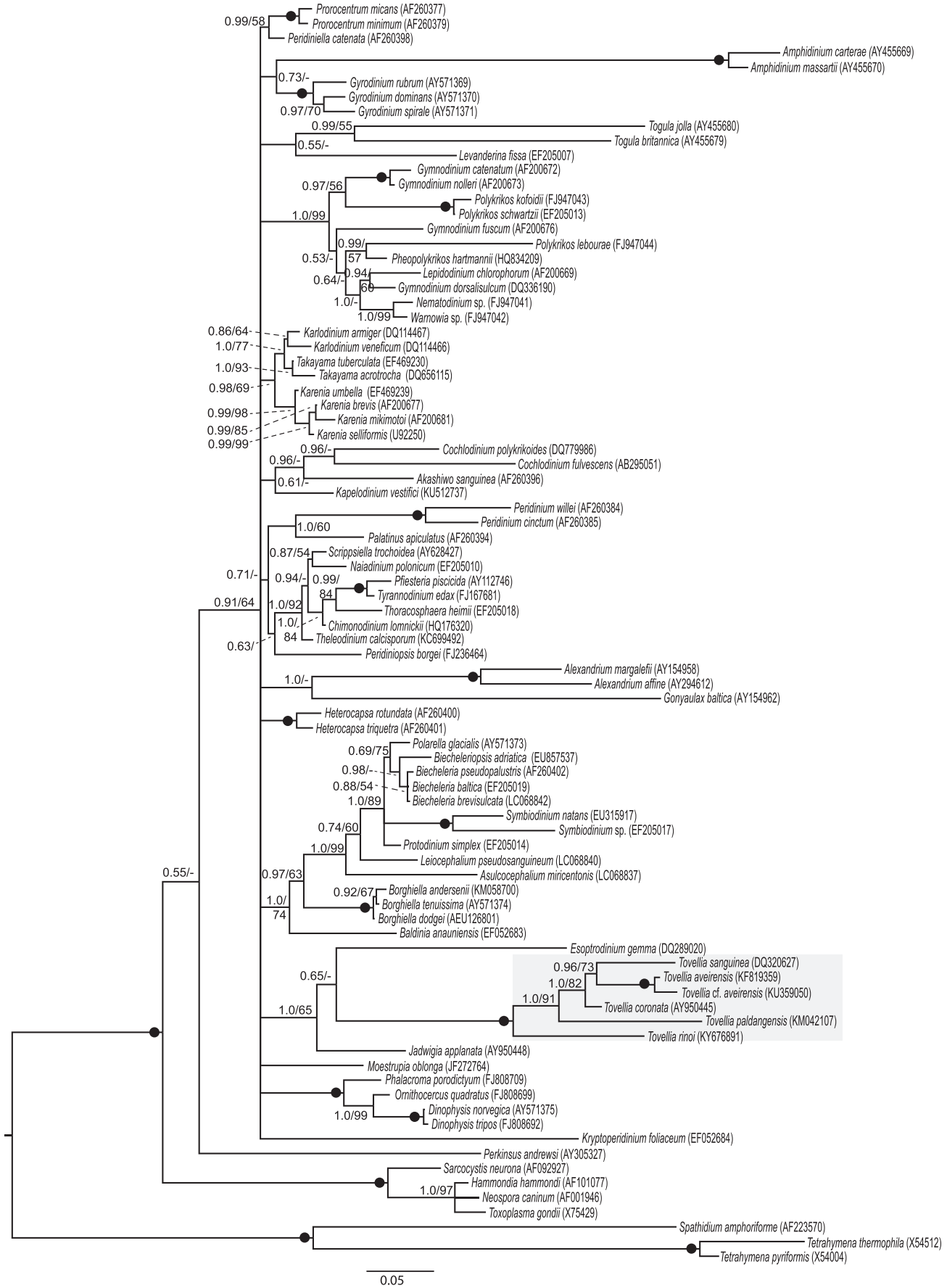

Fig. 73. Molecular phylogeny of *Tovellia rinoi* based on nuclear-encoded (partial) LSU rDNA (1151 base pairs) and analysed using Bayesian analysis. An out-group comprising three ciliates, four apicomplexans and *Perkinsus* was used to polarise the diverse assemblage of

T. nygaardii is closer to the cell middle than that of *T. rinoi* (Christen 1958; Li *et al.* 2015). The resting cyst of *T. nygaardii* was described as bipolar, with the equatorial constriction and axial projections that made it resemble the cyst type of *T. coronata* and supported the classification of the species in *Tovellia* (Christen 1958; Lindberg *et al.* 2005). In contrast, resting cysts of *T. rinoi* do not have axial projections and seem closer in general morphology to those of *T. aveirensis*, *T. paldangensis* or even the recently transferred *T. dodgei* (Sarma & Shyam) K.N.Mertens & H.Gu (Sarma & Shyam 1974; Pandeirada *et al.* 2014; Li *et al.* 2015; Luo *et al.* 2016). However, the resting cyst of *T. paldangensis* has only a few short spines (Li *et al.* 2015). The dense cover of thin spines on the resting cysts of *T. rinoi* is very distinctive, even from these closer types, and may be regarded as a novel resting cyst morphology in the family Tovelliaceae.

The phylogenetic position retrieved for *T. rinoi*, that is, forming a statistically well-supported sister group to the other *Tovellia* species included in the analysis, seems to match the different morphology of its resting cyst. However, the distance from other members of the Tovelliaceae clade (Fig. 73) is much greater than the distance from other *Tovellia* species, supporting the generic assignment. The phylogenetic position of *Opisthoaulax* is presently uncertain; the swimming cells show a much larger epicone than hypocone, suggestive of *Bernardinium*/*Esoptrodinium*, but the resting cyst displays features that recall *Tovellia* cysts with pointed axial horns (Calado *et al.* 2006; Calado 2011). Phylogenetic analyses of *Opisthoaulax* based on DNA sequences are needed to clarify its affinities.

As the amphiesmal composition of small species of *Tovellia* is very difficult to discern in live cells, we extended the search for similar forms to described species of *Gymnodinium* with a well-marked eyespot. *Gymnodinium wawrikae* J.Schiller (1955) is remarkably similar to *T. rinoi*, especially as depicted by Javornický (1967). However, both Schiller's and Javornický's specimens were slightly larger than the average specimens of *T. rinoi*, the cingulum was almost perfectly circular in *G. wawrikae* and Javornický remarked that cells lost their shape after some time under the microscope 'without leaving any membrane' (Javornický 1967, p. 58), which seems incompatible with the amphiesmal type of a *Tovellia*. Schiller's (1955) original illustrations of *G. wawrikae* further differ from both *T. rinoi* and Javornický's (1967, figs 1–4) drawings by showing cells with a hypocone somewhat longer than the epicone.

Asexual reproduction and gamete formation

The batches of *T. rinoi* cultures have maintained the ability to reproduce both asexually and sexually, with abundant production of resting cysts. This allowed for observations on reproductive processes comparable in detail with those published for *T. apiculata* (Stosch) Moestrup, K.Lindberg & Daugbjerg (Stosch 1973). Asexual reproduction was noted for *T. apiculata*, *T. aveirensis*, *T. coronata*, *T. dodgei*, *T. nygaardii* and *T. stoschii*, but the process was described in some detail only for *T. apiculata* and *T. aveirensis* (Wołoszyńska 1917; Christen 1958; Stosch 1973; Sarma & Shyam 1974; Shyam & Sarma 1976; Pandeirada *et al.* 2014). The report of the division of *T. dodgei* cells in the motile stage contrasts with the prevalence in other species of *Tovellia* of immotile division cysts that yield two to eight daughter cells (Sarma & Shyam 1974). Different modes of cell division between species classified in *Woloszynskia* were among the features that led Stosch (1973) to suggest that the genus was polyphyletic. However, the affinity of *T. dodgei* to other species of *Tovellia* is suggested by the described eyespot and resting cyst morphology (Luo *et al.* 2016). In addition, a greater diversity than previously realised in the division modes within a single dinoflagellate species has been recently documented (Figueroa & Bravo 2005; Hansen & Flaim 2007; Figueroa *et al.* 2008; Daugbjerg *et al.* 2014). Additional observations on *T. dodgei* are needed to clarify the amphiesmal features and the genetic relationship of the species.

The formation of division cysts in *T. rinoi* and the subsequent production and release of daughter cells were essentially similar to that described for *T. apiculata* and *T. aveirensis* (Stosch 1973; Pandeirada *et al.* 2014). The production of small cells both by sequential divisions separated by a short interphasis (termed 'depauperating divisions' by Stosch 1964, 1973) and through direct division into eight cells was described for *T. apiculata* (Stosch 1973). It was here shown for *T. rinoi* that even the smallest, lightly pigmented cells were capable of growing and dividing; however, only these small cells were involved in the 'dancing groups' from where fusing pairs emerged, which highlights reduction of cell size as an essential step in gamete differentiation.

Gamete fusion

Putative gametes of *T. rinoi* often carried on their mid-ventral face a hyaline protuberance that appears to correspond to the globose extension seen by SEM on the ventral ridge. Early fusing gametes were seen to connect through a hyaline bridge at the mid-ventral level, suggesting that the ventral protuberance plays a role in the initial attachment of gametes. The hyaline bridge observed in *T. rinoi* fusing gametes corresponds to the 'copulation globule' observed in initial stages of gamete fusion in *T. apiculata* and *Biecheleria pseudopalustris* (J.Schiller) Moestrup, K.Lindberg & Daugbjerg (Stosch 1973). Similar structures have been described from dinoflagellates of different groups (e.g. Spector *et al.* 1981; Litaker *et al.* 2002), and ventral globules have been documented by SEM in putative gametes of *Polykrikos kofoidii* Chatton and in the suessiacean species *Asulcocephalium miricentonis* Kazuya Takahashi, Moestrup & Iwataki and *Leiocephalium pseudosanguineum* Kazuya Takahashi, Moestrup & Iwataki (Tillmann & Hoppenrath 2013; Takahashi *et al.* 2015). A round protuberance documented by SEM near the apical area of

←
dinoflagellates (48 genera and 76 species). Numbers at internal nodes are posterior probabilities ($\geq$ 0.5) from Bayesian analysis followed by bootstrap values ($\geq$ 50%) from ML with 1000 replications. Bootstrap values below 50% are indicated by a '-'. Black circles indicate the highest possible support in Bayesian and ML analyses (1.0 and 100%, respectively). GenBank accession numbers are written in parentheses. The family Tovelliaceae with eyespot type C *sensu* Moestrup & Daugbjerg (2007) is indicated by a grey rectangle. Branch lengths are proportional to the number of character changes.

some cells of *Ostreopsis* cf. *ovata* Fukuyo was also hypothesised to be involved in sexual fusion (Accoroni *et al.* 2014).

After the initial stages of attachment, fusing gametes of *T. rinoi* swam for most of the fusion process, and the two gametes played different roles, one driving the swimming pair and the other appearing to progressively fuse into its partner. Comparable observations were made for *T. apiculata*: the wording "the lower left side of one gamete fuses into the upper right side of the other, while both ventral faces are turned in the same direction with respect to each other" (Stosch 1973, p. 116) is compatible with the sequences shown in Figs 49–60. In both *T. apiculata* and *T. rinoi*, the eyespots converge and eventually merge as a result of the rotation of the upper gamete until both gametes face the same direction and the gametic longitudinal flagella become the two longitudinal flagella of the planozygote (Stosch 1973). The fate of the gametic transverse flagella and the origin of the transverse flagellum of the planozygote remain unclear for both species.

Development of planozygotes and chromatic reduction

Observations of planozygotes of *Tovellia* developing into resting cysts were reported for *T. apiculata*, *T. coronata* and *T. aveirensis* (Stosch 1973; Lindberg *et al.* 2005; Pandeirada *et al.* 2014). Additionally, some information was given for the maturing cyst of *T. dodgei* without clear identification of the cell from which it originated (Sarma & Shyam 1974). The general differentiation of resting cysts in dinoflagellates involves the deposition of one or more wall layers directly around the cytoplasm and underneath the amphiesma, which is usually dissociated from the cytoplasm at that stage (Kokinos & Anderson 1995; Bravo & Figueroa 2014). The process observed in *T. rinoi* followed this pattern. However, the forming cyst of *T. rinoi* usually emerged from the discarded amphiesma before forming the spiny cover; whereas, smooth resting cysts may complete maturation still surrounded by the old cell cover, as described for *T. apiculata* (Stosch 1973) and commonly found in many peridinioids (e.g. Lefèvre 1932; Craveiro *et al.* 2011). In contrast to the commonly observed exclusion of the outer cell cover (which presumably includes at least the outer layers of the former amphiesma) from the resting cyst wall, TEM observations led to the suggestion that amphiesmal plates of the planozygote were used in the resting cyst wall of *Gymnodinium tylotum* Mapletoft, M.Montgomery, J.Waters & P.Wells (Bibby & Dodge 1972, as *Woloszynskia tylota*).

As an alternative to developing into resting cysts, planozygotes of *T. rinoi* were also observed to form division cysts from where swimming cells emerged. This has not been previously reported for planozygotes of *Tovellia*. However, recent observations of planozygotes of *T. aveirensis* revealed that they also can transform into division cysts that produce two swimming cells (Pandeirada *et al.*, unpublished). Planozygote division has been reported from a number of dinoflagellates, and recent work is changing the view that planozygote division is an uncommon, alternative route to encystment and showing that it may be much more significant in the life cycle of dinoflagellates (Uchida *et al.* 1996; Parrow & Burkholder 2004; Figueroa *et al.* 2010b, 2015). In particular, it has been suggested that it may promote faster genetic recombination by skipping the dormancy period of cysts (Figueroa *et al.* 2010b, 2015). This would be a valuable response to unfavourable conditions, hypothetically triggered by signals like differences in cell density, possibly perceived by cell contact frequency, variations of nutrient and light levels or the presence of parasites (Uchida *et al.* 1996; Uchida 2001; Figueroa *et al.* 2010b, 2015). It is not known what determined *T. rinoi* cells to divide rather than encyst, but the observed cell division, not encystment, in all cases where mating cells were isolated into a culture well with fresh medium, is not readily interpretable as a response to unfavourable conditions. Further experimentation is required before we may begin to understand the factors that determine the fate of planozygotes.

The large differences in numbers of resting cysts produced in batches originating from individual gamete-like cells, as well as from cells derived from the division of cyst-germinated cells, all grown under similar conditions, suggest that genetic differentiation occurs during some of the steps leading to the formation of these cells. Genetic recombination during meiosis may provide the mechanism whereby the different tendencies for cyst formation arise. An analogous involvement of meiosis in switches between homothally and heterothally has been described for *Gymnodinium catenatum* H.W. Graham (Figueroa *et al.* 2010a). Chromatic reduction in the life cycle of *T. rinoi* is expected to take place between the planozygote and the gamete stages. With the possible exception of the apparently diploid *Noctiluca scintillans* (Macartney) Kofoid (Zingmark 1970; Fukuda & Endoh 2006), the life cycle of dinoflagellates is regarded as predominantly haploid. Correspondingly, meiosis has been reported or assumed to take place or begin at the division of the planozygote, of the resting cyst or of a single cell emerged from the resting cyst (usually called planomeiocyte) (Stosch 1973; Pfiester 1975; Litaker *et al.* 2002; Parrow & Burkholder 2003, 2004; Figueroa *et al.* 2010b). However, the well-known chromosomal arrangements of the two-step meiotic division typical of most eukaryotic groups are not found in dinoflagellates, and recognition of meiosis is therefore difficult. A two-step meiosis was demonstrated for *Prorocentrum micans* Ehrenberg by microspectrofluorometry of nuclei stained with ethidium bromide, which showed at the onset of meiosis an increase from two to four times the DNA content of nuclei formed after the second meiotic division (Bhaud *et al.* 1988). Whether a two-step chromatic reduction is a general feature among dinoflagellates, as opposed to a single-step halving of chromosome numbers (i.e. by a single nuclear division not preceded by DNA replication; see Himes & Beam 1975), remains undemonstrated, making an interpretation of ploidy levels in cells produced in pairs from a planozygote or a resting cyst uncertain. Following the seminal paper by Stosch (1972), the most conspicuous morphological marker for the occurrence of meiosis in some dinoflagellates is nuclear cyclosis, during which the nuclear contents rotate in what is interpreted as preparation and beginning of prophase I. However, nuclear cyclosis is not a universal feature among dinoflagellates (e.g. Pfiester 1975; Figueroa *et al.* 2015) and was not detected at any stage of the life cycle of *T. rinoi*. The occurrence of two longitudinal flagella in planomeiocytes that displayed nuclear cyclosis after swimming away from a parent resting cyst may indicate that paired longitudinal flagella are a marker for a diploid nucleus ready to undergo meiosis; paired longitudinal

flagella were not found in cells originating from the resting cysts of *T. rinoi*, suggesting that meiosis occurred or at least started before their formation. However, direct evidence for the occurrence of meiosis in *T. rinoi* is still lacking, and further studies are required to determine the exact location and mechanism of chromatic reduction in this species.

ACKNOWLEDGEMENTS

M.S.P. and S.C.C. were supported by grants SFRH/BD/109016/2015 and SFRH/BPD/68537/2010, respectively, from the financing programs POCH (Programa Operacional Capital Humano) and QREN, POPH, Tipologia 4.1, Formação Avançada, and by the European Social Funding (FSE) and the Portuguese Ministry of Education and Science (MEC). GeoBioTec (UID/GEO/04035/2013) supported this project. For molecular work we used the facilities at the Laboratory of Molecular Studies for Marine Environments (LEMAM), Univ. Aveiro, Portugal.

REFERENCES

Accoroni S., Romagnoli T., Pichierri S. & Totti C. 2014. New insights on the life cycle stages of the toxic benthic dinoflagellate *Ostreopsis* cf. *ovata*. *Harmful Algae* 34: 7–16.

Bhaud Y., Soyer-Gobillard M.-O. & Salmon J.M. 1988. Transmission of gametic nuclei through a fertilization tube during mating in a primitive dinoflagellate, *Prorocentrum micans* Ehr. *Journal of Cell Science* 89: 197–206.

Bibby B.T. & Dodge J.D. 1972. The encystment of a freshwater dinoflagellate: a light and electron-microscopical study. *British Phycological Journal* 7: 85–100.

Bravo I. & Figueroa R.I. 2014. Towards an ecological understanding of dinoflagellate cyst functions. *Microorganisms* 2: 11–32.

Calado A.J. 2011. On the identity of the freshwater dinoflagellate *Glenodinium edax*, with a discussion on the genera *Tyrannodinium* and *Katodinium*, and the description of *Opisthoaulax* gen. nov. *Phycologia* 50: 641–649.

Calado A.J., Craveiro S.C., Daugbjerg N. & Moestrup Ø. 2006. Ultrastructure and LSU rDNA-based phylogeny of *Esoptrodinium gemma* (Dinophyceae), with notes on feeding behavior and the description of the flagellar base area of a planozygote. *Journal of Phycology* 42: 434–452.

Christen H.R. 1958. *Gymnodinium Nygaardi* sp. nov. *Berichte der Schweizerischen Botanischen Gesellschaft* 68: 44–49.

Craveiro S.C., Calado A.J., Daugbjerg N., Hansen G. & Moestrup Ø. 2011. Ultrastructure and LSU rDNA-based phylogeny of *Peridinium lomnickii* and description of *Chimonodinium* gen. nov. (Dinophyceae). *Protist* 162: 590–615.

Darriba D., Taboada G.L., Doallo R. & Posada D. 2012. jModelTest 2: more models, new heuristics and parallel computing. *Nature Methods* 9: 772.

Daugbjerg N., Hansen G., Larsen J. & Moestrup Ø. 2000. Phylogeny of some of the major genera of dinoflagellates based on ultrastructure and partial LSU rDNA sequence data, including the erection of three new genera of unarmoured dinoflagellates. *Phycologia* 39: 302–317.

Daugbjerg N., Andreasen T., Happel E., Pandeirada M.S., Hansen G., Craveiro S.C., Calado A.J. & Moestrup Ø. 2014. Studies on woloszynskioid dinoflagellates VII. Description of *Borghiella andersenii*: light and electron microscopy and phylogeny based on LSU rDNA. *European Journal of Phycology* 49: 436–449.

Figueroa R.I. & Bravo I. 2005. Sexual reproduction and two different encystment strategies of *Lingulodinium polyedrum* (Dinophyceae) in culture. *Journal of Phycology* 41: 370–379.

Figueroa R.I., Bravo I. & Garcés E. 2008. The significance of sexual versus asexual cyst formation in the life cycle of the noxious dinoflagellate *Alexandrium peruvianum*. *Harmful Algae* 7: 653–663.

Figueroa R.I., Rengefors K., Bravo I. & Bensch S. 2010a. From homothally to heterothally: mating preferences and genetic variation within clones of the dinoflagellate *Gymnodinium catenatum*. *Deep-Sea Research II* 57: 190–198.

Figueroa R.I., Garcés E. & Camp J. 2010b. Reproductive plasticity and local adaptation in the host-parasite system formed by the toxic *Alexandrium minutum* and the dinoflagellate parasite *Parvilucifera sinerae*. *Harmful Algae* 10: 56–63.

Figueroa R.I., Dapena C., Bravo I. & Cuadrado A. 2015. The hidden sexuality of *Alexandrium minutum*: an example of overlooked sex in dinoflagellates. *PloS ONE* 10 (11): e0142667. DOI:10.1371/journal.pone.0142667.

Fukuda Y. & Endoh H. 2006. New details from the complete life cycle of the red-tide dinoflagellate *Noctiluca scintillans* (Ehrenberg) McCartney [sic]. *European Journal of Protistology* 42: 209–219.

Guindon S., Dufayard J.F., Lefort V., Anisimova M., Hordijk W. & Gascuel O. 2010. New algorithms and methods to estimate maximum-likelihood phylogenies: assessing the performance of PhyML 3.0. *Systematic Biology* 59: 307–321.

Hansen G. & Flaim G. 2007. Dinoflagellates of the Trentino Province, Italy. *Journal of Limnology* 66: 107–141.

Himes M. & Beam C.A. 1975. Genetic analysis in the dinoflagellate *Crypthecodinium* (*Gyrodinium*) *cohnii*: evidence for unusual meiosis. *Proceedings of the National Academy of Sciences of the United States of America* 72: 4546–4549.

Javornický P. 1967. Some interesting algal flagellates. *Folia Geobotanica et Phytotaxonomica* 2: 43–67, pls 2–9.

Kokinos J.P. & Anderson D.M. 1995. Morphological development of resting cysts in cultures of the marine dinoflagellate *Lingulodinium polyedrum* (=*L. machaerophorum*). *Palynology* 19: 143–166.

Kremp A. 2013. Diversity of dinoflagellate life cycles: facets and implications of complex strategies. In: *Biological and geological perspectives of dinoflagellates* (Ed. by J.M. Lewis, F. Marret & L. Bradley), pp. 197–205. The Micropaleontological Society, Special Publications. Geological Society, London.

Lefèvre M. 1932. Monographies des espèces d'eau douce du genre *Peridinium*. *Archives de Botanique, Mémoires* 2 (mémoire 5): 1–210, pls 1–6.

Lenears G., Maroteaux L., Michot B. & Herzog M. 1989. Dinoflagellates in evolution. A molecular phylogenetic analysis of large subunit ribosomal RNA. *Journal of Molecular Evolution* 29: 40–51.

Li Z., Shin H.H. & Han M.-S. 2015. Morphology and phylogeny of a new woloszynskioid dinoflagellate *Tovellia paldangensis* sp. nov. (Dinophyceae). *Phycologia* 54: 67–77.

Lindberg K., Moestrup Ø. & Daugbjerg N. 2005. Studies on woloszynskioid dinoflagellates I: *Woloszynskia coronata* re-examined using light and electron microscopy and partial LSU rDNA sequences, with description of *Tovellia* gen. nov. and *Jadwigia* gen. nov. (Tovelliaceae fam. nov.). *Phycologia* 44: 416–440.

Litaker R.W., Vandersea M.W., Kibler S.R., Madden V.J., Noga E.J. & Tester P.A. 2002. Life cycle of the heterotrophic dinoflagellate *Pfiesteria piscicida* (Dinophyceae). *Journal of Phycology* 38: 442–463.

Luo Z., You X., Mertens K.N. & Gu H. 2016. Morphological and molecular characterization of *Tovellia* cf. *aveirensis* (Dinophyceae) from Jiulong River, China. *Nova Hedwigia* 103: 79–94.

Moestrup Ø. & Daugbjerg N. 2007. On dinoflagellate phylogeny and classification. In: *Unravelling the algae, the past, present, and future of algal systematics* (Ed. by J. Brodie & J. Lewis), pp. 215–230. CRC Press, Boca Raton, FL (Systematics Association Special Volume No. 75).

Nichols H.W. 1973. Growth media – freshwater. In: *Handbook of phycological methods. Culture methods & growth measurements* (Ed. by J.R. Stein), Cambridge, United Kingdom: Cambridge University press, pp. 7–24.

Nunn G.B., Theisen B.F., Christensen B. & Arctander P. 1996. Simplicity-correlated size growth of the nuclear 28S ribosomal RNA D3 expansion segment in the crustacean order Isopoda. *Journal of Molecular Evolution* 42: 211–223.

Pandeirada M.S., Craveiro S.C. & Calado A.J. 2013. Freshwater dinoflagellates in Portugal (W Iberia): a critical checklist and new observations. *Nova Hedwigia* 97: 321–348.

Pandeirada M.S., Craveiro S.C., Daugbjerg N., Moestrup Ø. & Calado A.J. 2014. Studies on woloszynskioid dinoflagellates VI: description of *Tovellia aveirensis* sp. nov. (Dinophyceae), a new species of Tovelliaceae with spiny cysts. *European Journal of Phycology* 49: 230–243.

Parrow M.W. & Burkholder J.M. 2003. Estuarine heterotrophic cryptoperidiniopsoids (Dinophyceae): life cycle and culture studies. *Journal of Phycology* 39: 678–696.

Parrow M.W. & Burkholder J.M. 2004. The sexual life cycles of *Pfiesteria piscicida* and cryptoperidiniopsoids (Dinophyceae). *Journal of Phycology* 40: 664–673.

Pfiester L.A. 1975. Sexual reproduction of *Peridinium cinctum* f. *ovoplanum* (Dinophyceae). *Journal of Phycology* 11: 259–265.

Ronquist F. & Huelsenbeck J.P. 2003. MrBayes 3: Bayesian phylogenetic inference under mixed models. *Bioinformatics* 19: 1572–1574.

Sarma Y.S.R.K. & Shyam R. 1974. On the morphology, reproduction and cytology of two new freshwater dinoflagellates from India. *British Phycological Journal* 9: 21–29.

Schiller J. 1955. Untersuchungen an den planktischen Protophyten des Neusiedlersees 1950–1954, I. Teil. *Wissenschaftliche Arbeiten aus dem Burgenland* 9: 1–66, pls I–XIII.

Scholin C.A., Herzog M., Sogin M. & Anderson D.M. 1994. Identification of group- and strain-specific genetic markers for globally distributed *Alexandrium* (Dinophyceae). II. Sequence analysis of a fragment of the LSU rRNA gene. *Journal of Phycology* 30: 999–1011.

Shyam R. & Sarma Y.S.R.K. 1976 ('1975'). *Woloszynskia stoschii* and *Gymnodinium indicum*, two new freshwater dinoflagellates from India: morphology, reproduction and cytology. *Plant Systematics and Evololution* 124: 205–212.

Spector D.L., Pfiester L.A. & Triemer R.E. 1981. Ultrastructure of the dinoflagellate *Peridinium cinctum* f. *ovoplanum* II. Light and electron microscopic observations on fertilization. *American Journal of Botany* 68: 34–43.

Stosch H.A. 1964. Zum Problem der sexuellen Fortpflanzung in der Peridineengattung *Ceratium*. *Helgoländer Wissenschaftliche Meeresuntersuchungen* 10: 140–152.

Stosch H.A. 1972. La signification cytologique de la 'cyclose nucléaire' dans le cycle de vie des Dinoflagellés. *Mémoires Publiés par la Société Botanique de France* 1972: 201–212. [Colloque sur les cycles sexuels el l'alternance des générations chez les Algues. Paris, 1970.]

Stosch H.A. 1973. Observations on vegetative reproduction and sexual life cycles of two freshwater dinoflagellates, *Gymnodinium pseudopalustre* Schiller and *Woloszynskia apiculata* sp. nov. *British Phycological Journal* 8: 105–134.

Swofford D.L. 2003. PAUP*: phylogenetic analysis using parsimony (*and other methods), version 4.0b10. Sinauer Associates, Sunderland, MA.

Takahashi K., Moestrup Ø., Jordan R.W. & Iwataki M. 2015. Two new freshwater woloszynskioids *Asulcocephalium miricentonis* gen. et sp. nov. and *Leiocephalium pseudosanguineum* gen. et sp. nov. (Suessiaceae, Dinophyceae) lacking an apical furrow apparatus. *Protist* 166: 638–658.

Tillmann U. & Hoppenrath M. 2013. Life cycle of the pseudocolonial dinoflagellate *Polykrikos kofoidii* (Gymnodiniales, Dinoflagellata). *Journal of Phycology* 49: 298–317.

Uchida T. 2001. The role of cell contact in the life cycle of some dinoflagellate species. *Journal of Plankton Research* 23: 889–891.

Uchida T., Matsuyama Y., Yamaguchi M. & Honjo T. 1996. The life cycle of *Gyrodinium instriatum* (Dinophyceae) in culture. *Phycological Research* 44: 119–123.

Warns A., Hense I. & Kremp A. 2013. Modelling the life cycle of dinoflagellates: a case study with *Biecheleria baltica*. *Journal of Plankton Research* 35: 379–392.

Waterhouse A.M., Procter J.B., Martin D.M.A., Clamp M. & Barton G.J. 2009. Jalview version 2 – a multiple sequence alignment editor and analysis workbench. *Bioinformatics* 25: 1189–1191.

Wołoszyńska J. 1917. Nowe gatunki Peridineów, tudziez spostrzezenia nad budowa okrywy u Gymnodiniów i Glenodiniów. — Neue Peridineen-Arten, nebst Bemerkungen über den Bau der Hülle bei *Gymno-* und *Glenodinium*. *Bulletin International de l'Academie des Sciences de Cracovie, Classe des Sciences Mathématiques et Naturelles, série B: Sciences Naturelles* 1917: 114–122, pls 11–13.

Zingmark R.G. 1970. Sexual reproduction in the dinoflagellate *Noctiluca miliaris* Suriray. *Journal of Phycology* 6: 122–126.

Received 11 January 2017; accepted 8 March 2017